Proceedings of the 10o Brazilian Congress of Thermal Sciences and Engineering -- ENCIT 2004
Braz. Soc. of Mechanical Sciences and Engineering -- ABCM, Rio de Janeiro, Brazil, Nov. 29 -- Dec. 03, 2004

TURBULENT FORCED CONVECTION AIR COOLING OF ELECTRONICS

Mila Avelino[1]
Departamento de Engenharia Mecânica, Unversidade do Estado do Rio de Janeiro – UERJ, 20550-013 - Rio de Janeiro, RJ, Brazil
mila@uerj.br

Gustavo R. dos Anjos
Departamento de Engenharia Mecânica, Unversidade do Estado do Rio de Janeiro – UERJ, 20550-013 - Rio de Janeiro, RJ, Brazil
gustavo.rabello@terra.com.br

Sadik Kakaç
Department of Mechanical Engineering, University of Miami, Coral Gables, FL, USA
skakac@coeds.eng.miami.edu

Abstract. *Air cooling is still the dominant method for dissipating the heat produced by electronic components. In a typical electronic device, the components are situated on a Printed Circuit Board (PCB). For most applications natural convection is sufficient to cool the components. However in some cases forced convection air cooling, which provides more effective cooling, has to be used. The size of the components is often considerably smaller than the PCB. Since the air flow is seeking the path of least resistance, the geometry of the electronic components is of major importance. This air flow pattern has a major impact on the performance of the heat dissipation, why knowledge of the flow pattern is of vital importance. The aim of this work has been to investigate the influence of flow pattern on the performance of heat exchange used for electronics cooling. The focus has been set on determining the parameters that influence the geometry, and to quantify their relative importance using experimental and numerical techniques. Experimental and numerical parametric studies are presented. The influence of the array arrangement over the plate as well as the dimensions and air velocity, on the thermal and hydraulic performance have been investigated. The flow was turbulent, and the measurements have been performed in a wind tunnel. Numerical predictions have been performed by using two different numerical schemes: a parabolic differential scheme and a* k-ε *model used for integrating Reynolds-Average Navier-Stokes (RANS) equations and the continuity equation. For turbulence modeling wall functions that take into account turbulent wall shear stress and turbulent heat fluxes are used to specify the boundary conditions. The experimental data can be used to validate the numerical model, which in turn can be used for parametric studies. The parameterization uses the displacement in origin concept for the velocity and the temperature fields.*

Keywords*. forced convection, heat transfer, pressure drop, air cooling, electronics*

1. Introduction

With the advent of high-density microelectronic devices, the power dissipation of very large scale integrated (VLSI) circuits is becoming a critical concern. The continuing decrease in feature size and the corresponding increase in chip density and operating frequency in microelectronic circuits have made overheating a major concern in VLSI design. Effective thermal design has been investigated together with accurate and efficient power estimation. Recently, with existing heat flux levels exceeding 100 W/cm^2, new thermal control methods have become mandatory, and a variety of power estimation techniques have been proposed to manage the power of an Integrated Circuit (IC) design.

Computer-Aided Design (CAD) tools are needed to help with the power management tasks. Indeed, development of efficient cooling techniques for ICs chips is one of the important contemporary applications of microscale heat transfer. Microchannel heat sinks are the ultimate solution for removing these high amounts of heat. This pressing requirement has initiated extensive research in microchannel cooling. Experimental and analytic methods are reported for predicting the flow and temperature of the coolant, which is essential for chip thermal design Bayazitogly(2003).

Cooling of electronics has received much attention due to their ultimate potential for cooling high power microelectronic and application in biomechanical and aerospace industries. Heat dissipation from micro devices is now becoming a cutting edge field since the performance of the device. It is used is primarily determined by flow and temperature fields. Geometric parameters influence significantly on the convective heat transfer characteristics.

Recent advances in micromechanics allow the fabrication of various micron scale devices, Fig. 1. These micron scale devices can find their applications, both in commercial products and scientific investigations. However, it has been reported that the fluid behavior in such an extremely small scale deviates from the predictions based on the continuum hypotheses, which have been generally accepted in the macro phenomena, Herwig (2002,2003). This deviation is due to the rarefaction and compressibility effects mainly due to the dimensions of microelectronic devices.

Microelectricalmechanical systems (MEMS) are the subject of increasing active research in a widening field of disciplines. In this range of machine scale, the dynamic behavior of the fluid motion against fluid and thermal drags cannot be predicted with the continuum theory. Thus, many researchers have responded in various ways, such as by proposing power estimation techniques, Brodersen(1991) and Chandrakasan(1992).

---

[1] Correspondence Author

While it is highly desirable, high-level power estimation is also inevitably inaccurate, or approximate. The need to obtain some fundamental understanding of heat and fluid flow in micromechanical devices has been identified as a critical technological phenomenon. Indeed, the power estimation problem has received much more attention in the literature, and many estimation techniques at this level have been proposed.

Navier-Stokes-based fluid dynamics solvers are often inaccurate when applied to MEMS. This inaccuracy stems from their calculation of molecular transport effects, such as viscous dissipation and thermal conduction, from bulk flow quantities, such as mean velocity and temperature. This approximation of micro-scale phenomena with macro-scale information fails as the characteristic length of the gaseous flow gradients (L) approaches the average distance traveled by molecules between collisions (the mean path, λ). The ratio of these quantities is known as Knudsen number ($Kn=\lambda/L$). For $Kn<0.01$, the flow is considered to be in the "continuum" regime. As Kn increases, the flow moves through the slip-flow ($0.01<Kn<0.1$) and the "transition" ($0.1<Kn<3$) regimes and finally enters the "free-molecular" ($Kn>3$) regime, each requiring a particular type of analysis, Table 1. Knudsen (1909) and Tunc and Bayazitogly(2002).

Table 1 – Regimes according to Knudsen number.

Knudsen number ($Kn=\lambda/L$)	**Flow Regime**
$Kn<0.01$	"Continuum" regime
$0.01<Kn<0.1$	Slip-flow regime
$0.1<Kn<3$	"Transition" regime
$Kn>3$	"Free-molecular" regime

Liquid flow and heat transfer in microchannels are critical to the design and process control of various Microelectricalmechanical Systems (MEMS) and biomedical lab-on-a-chip devices. Experimental studies in the literature have shoed that many microchannel flow and heat transfer phenomena cannot be explained by conventional theories of transport phenomena. For instance, the transition from laminar flow to turbulent flow starts much earlier (e.g., from Re=300); the correlations between the friction factor and the Reynolds number for microchannel flow are very different from that in classical theory of fluid mechanics; the apparent viscosity and the friction factor of a liquid flowing through a microchannel may be several times higher than that in the conventional theories. Therefore, fundamental understanding of liquid flow and convection heat transfer in microchannels is required. Gad-el-Hak(2002,2003).

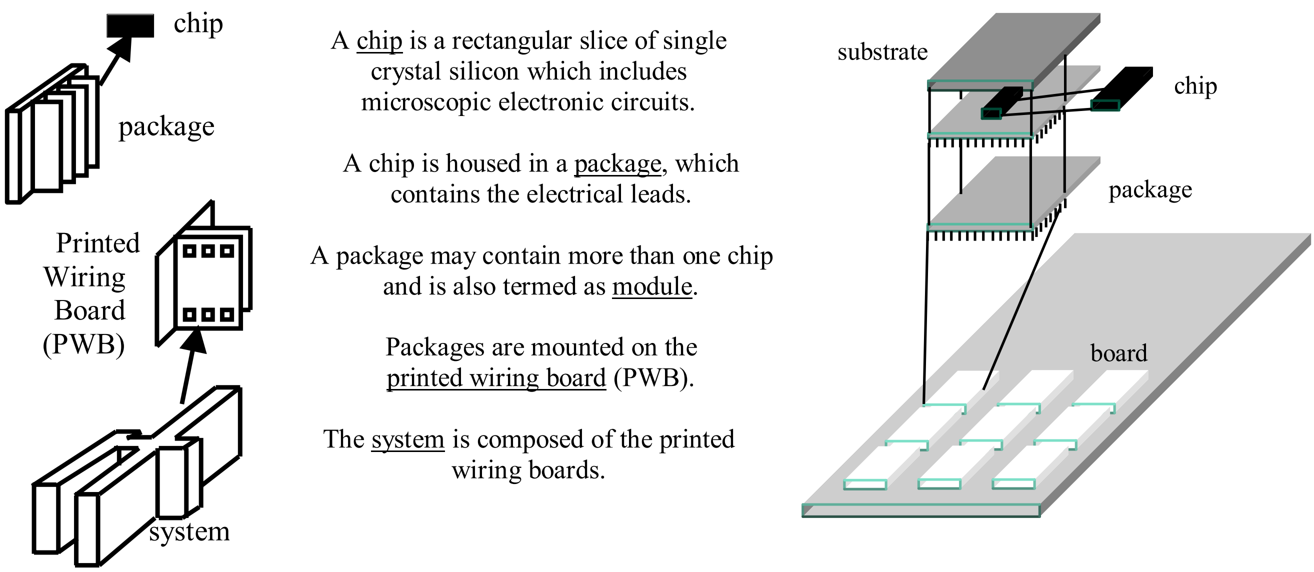

Figure 1 – Schematic assembling of a microprocessor

These special characteristics of flows and heat transfer in microchannels are the results of microscale channel size and the interfacial electrokinetic and surface roughness effects near the solid-liquid interface, where the interface represents the wall of the microscale flow channel. These effects will significantly affect both the liquid flow and the convective heat transfer. Karniadakis and Beskok(2002).

Gaseous flow studies were carried out for the slip flow conditions where although continuum assumption is not valid due to the rarefaction effect, Navier-Stokes can still be applied with some modifications at the boundary. Typically, microchannel boundary conditions that are applied to fluid flow and heat transfer equations, gas velocity and temperature, are equivalent to the corresponding wall values. On the other hand, these conditions are not held for rarefied gas flow in microchannels. Not only does the fluid slip along the wall with a finite tangential velocity, but there is also a jump between wall with and fluid temperatures.

It has became a common practice to assemble a large number of chips on a single multilayer ceramic module and, in turn, to assemble multiple modules on a single board. For large-scale computers, the heat removal from the chips is the major technical problem in achieving higher data processor speeds.

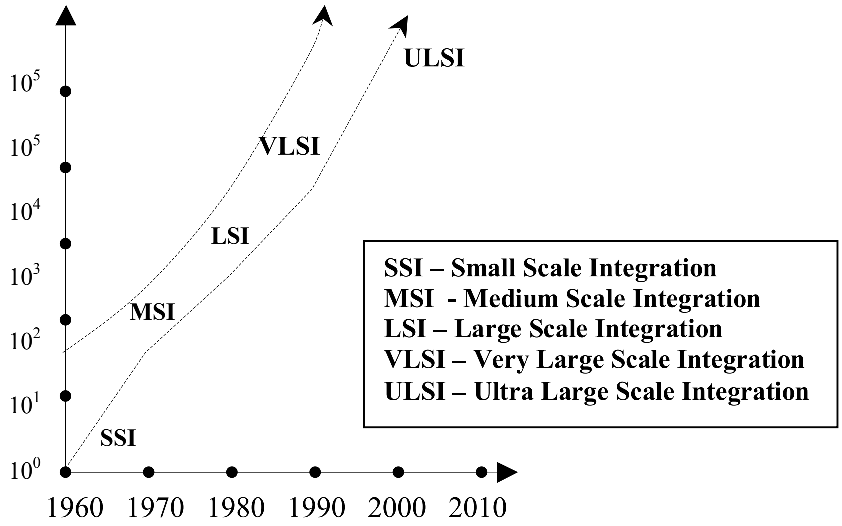

Figure 2 – Integrated circuits are classification by the number of transistors and other electronic components they contain and their growth rate since last decades.

Two dimensional assemblies are typical, however, three dimensional configuration are also being considered for yet lager packing densities. This general trend has accelerated drastically after 1970's with the introduction of LSI, VLSI and ULSI, Fig. 2.

In many of today's computers, power densities at the chip and module level are as large as 30 and 5 W/cm^2, respectively. Within less than a five-year period, researchers expect 10 million component on 1.25mm chip to be available. The power dissipation will be 100 W/cm^2 in the chip level and 25 W/cm^2 in the module level. The longer term project suggests 125 W/cm^2 for 50 million or a billion components depending upon the compromise between the switch power and the speed. This heat dissipation level is in the range of thermal loadings associated with nuclear blast.

The temperature is in excess of 1000^{o}C whereas for a successful thermal management of microelectronic components in the same heat flux range, maximum surface temperatures should be maintained between 50^{o}C and 100^{o}C. This must be obtained uniformly over the board and considering cost and reliable life restrictions.

For the fast developing electronic technology, it becomes more of a necessity for the people in fluid and thermal sciences and control technology to meet the needs of the microelectronic technology. This is a challenge to increase the reliability of the existing systems and to be able to develop smaller, faster and more reliable systems.

Cooling requirements in microelectronics are among the toughest barriers of to develop faster, smaller, and still more reliable systems. In the past three decades electronics has developed to surround all faces of modern life. At the same time, with increasing number of applications reliability has become a real crucial problem. Realizing the importance of the problem, much emphasis has been given to the improvement of the reliability level as well to the improvement of the electrical performances of the electronic devices. Improvement in the technology made it possible in early 1960's to integrate monolithic circuits on a silicon chip. This enabled electronic manufactures to build larger number of smaller chips on smaller circuit boards. In the last 35 years chip sizes reduced from approximately from 100 to 1 mm and the number of components in one chip increased approximately from 1 to 105.

The purpose of thermal design is: to provide equipment to remove the heat from heat sources to one or more heat sinks in the environment. The main goal of thermal control is: to maintain the temperatures of individual elements with their functional and maximum allowable limits.

The Functional Temperature Limit is the range in which the electronic element's performance is in accordance with the expectation of the electronic designer. If the operation temperature goes over the limit, degraded electrical performance and logic errors are very likely to occur. In order to meet the cooling requirements of microelectronics, the task of thermal design engineer is to find the most efficient thermal paths from the heat source to the ultimate heat sink. For this purpose, emphasis must be given to find ways of reducing both internal and external resistances.

The overall heat transfer can be enhanced largely through reducing internal resistance. Thermal resistances at this level are due to conduction through layers and contact surfaces between the layers. There are analytical solutions to various forced convection problems in ducts, but in most of cases they will not be applicable direct to electronic cooling. They will represent minimum values for heat transfer and can be used as a reference bottom value.

Local and average heat transfer coefficients for constant wall temperature and constant wall heat flux boundary conditions with unheated starting length, arbitrary temperature distribution and arbitrary heat flux distribution are available for laminar and turbulent boundary layer flows over a flat plate.

The cooling of electronic equipment has become very interesting research topic for heat transfer community. It has increased research collaboration between Universities and industry. The hardware design of electronic equipment is an interdisciplinary work which involves the integration of thermal electrical and manufacturing engineering.

Because of the complexibility of the packaging, it is difficult to rely only on numerical methods; experimental studies are important to validate the theoretical modeling. In some cases manufactures of electronic equipment are forced to rely heavily on experimental findings. Therefore, the practical methods for the determination of the parameters required for the thermal analysis of electronic systems, the various experiments methods for obtaining sufficiently accurate values for the heat transfer coefficient, effective thermal conductivity and the total thermal resistance are important topics in electronic cooling.

Good thermal management can be achieved through optimum design considerations as it is the case with every real engineering problem, including: Performance, Productivity, Servicivility, Compatibility and Cost.

2. Cooling Techniques

In Cooling of Electronic Components various methods have been employed with various coolant fluids:

1. Air Cooling – Natural Convection
2. Air Cooling – Forced Convection
3. Liquid Cooling (Including evaporation, boiling) direct or indirect
   - 3.1 Immersion – natural convection fluorocarbons
   - 3.2 Immersion– boiling fluorocarbons
   - 3.3 Water – forced convection

Air cooling is the most traditionally and still most used cooling technology. The main reason for that, probably, is the ready availability in the desired amounts, except in space applications. In addition, the simple design, low costs, easy maintenance and high reliability make air a good choice. Comparison of cooling of electronic components various methods are shown in Table 2.

Table 2 – Comparison of cooling of electronic components various methods.

	NAC	FAC	FAC	Liquid (Direct)	Liquid(Indirect)
Coolant	air	air	air, water	inert insulator liq	water etc.
Coolant Mover	buoyancy	fan/blower	fan/blower, pump	pump	pump
Coolant Velocity	0.2 m/s	0.5 –10m/s			
Cooling Capability	small	middle-large	middle-large	very large	large
Equipment Volume	large	middle	middle	small	small
Acoustic Noise	none	middle-large	middle	small	small
Reliability	high	middle	middle	small	small
Economy	high	middle-large	middle	small-middle	small-middle
Remarks (capabilities, etc.)	capability increases by chimney effect			capability depends on HE capability	He-gas used to decrease contact their resistance

Natural convection is used for low levels of power and packaging densities. With reduced noise level, low pressure drop, low power requirements and high reliability, this is an attractive solution. However, cooling of large scale equipment requires higher heat dissipation; therefore one must consider forced air convection in most of the cases. Higher heat transfer performance, ease and greater degree of control and insensitivity to packaging orientation are some of the advantages of the forced convection.

Large number of geometric variables is frequently encountered in the cooling of electronic equipment. Different sized in the flow passages which have the same diversity in the shape and size make it almost impossible to form a data base for accurate analysis. However, generic cooling problems and related flow configurations can be identified and some very useful correlations can be drawn from the careful numerical and experimental research.

For fluid flow though channels with an array of block-like modules, many studies have been done and many correlations are valid for laminar, turbulent or transitional flows: Forced Convection, Natural Convection, Mixed Convection. Heat will be transferred from a component surface to a cooling fluid stream by convection/radiation heat transfer. It may include flow over components on isolated surfaces or these components may be within two parallel channels usually at the top of the bottom plate. A certain fraction of the energy released in a component is removed by coolant. Correlations in terms of dimensionless numbers are important for design, but in cooling of electronic systems the problem is a practical geometrical parameters are so different from design to design and complex that it is difficult for the designer to use a correlation.

3. Methodology

Boundary conditions that take into account turbulent wall shear stress and turbulent heat fluxes are employed in two numerical methods. Elliptical Numerical Scheme – CAST and a Parabolic Numerical Solver. Detailed procedure of implementation and results can be found in Avelino(2002)

3.1. The Geometry Considered

Many existing forced air cooling systems consists of arrays of vertically or horizontally staked printed circuit cards carrying electronic modules, see Fig. 3. In all the cases, velocity boundary layer reaches a hot-rough surface, where the thermal boundary layer flow initiates, Fig. 4.

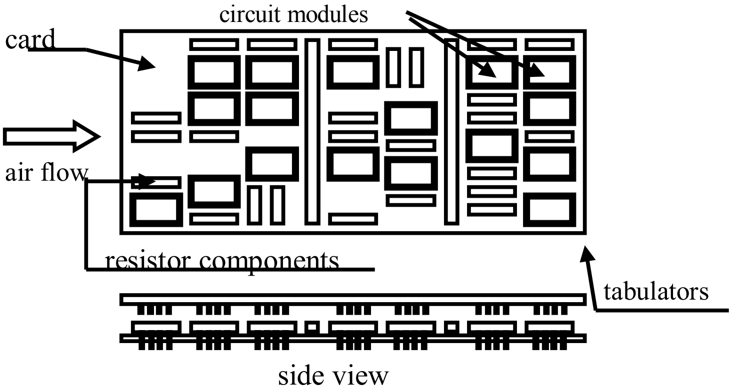

Figure 3 – Typical arrangements of air-cooled electronic modules on printed circuit card

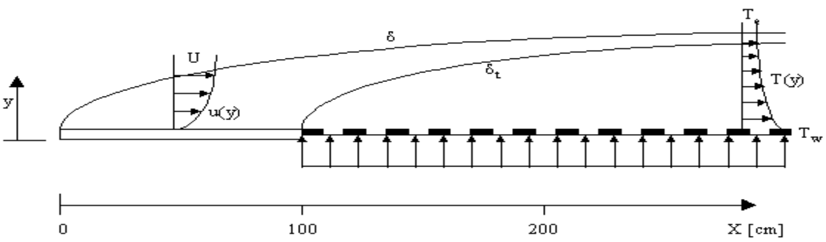

Figure 4 – Geometry of the test section.

3.2. The Governing Equations

The governing equations of the standard k-ε formulation, with the mean parts of the velocity and pressure fields denoted by u_i and p, respectively, and the fluctuation of the turbulent quantities denoted by dashes, can be cast as

$$\frac{\partial u_i}{\partial x_i} = 0, \tag{1}$$

$$\frac{\partial u_i}{\partial t} + u_j \frac{\partial u_i}{\partial x_j} = -\frac{1}{\rho} + \frac{\partial p}{\partial x_i} + \frac{\partial \tau_{ij}}{\partial x_j} + \frac{\partial}{\partial x_j}(\nu d_{ij}), \tag{2}$$

$$\rho c_p \frac{D\overline{T}}{Dt} = k\nabla^2 \overline{T} + \overline{\phi}, \tag{3}$$

where

$$\overline{\phi} = \tau_{ij} \frac{\partial u_i}{\partial x_j}. \tag{4}$$

Here, ρ is the density of the fluid. The Reynolds stresses, τ_{ij} is

$$\tau_{ij} = -\langle u_i' u_j' \rangle, \tag{5}$$

where the Dirac brackets denote time averaging. A summation is understood for repeated subscripts.

3.3. The Turbulence Model

The standard k-ε model relates the components of the Reynolds stress tensor to the mean flow gradients with the aid of the eddy viscosity concept

$$\tau_{ij} = -\frac{2}{3} k\delta_{ij} + \nu_t d_{ij} . \tag{6}$$

Here δ_{ij} is the Kroeneker delta; k, the turbulent kinetic energy, is given by

$$k = \frac{\langle u_i' u_j' \rangle}{2}, \tag{7}$$

ν_t is the eddy viscosity, ν the kinematic viscosity of the fluid and d_{ij} the velocity strain

$$d_{ij} = \frac{\partial u_i}{\partial x_j} + \frac{\partial u_j}{\partial x_i} . \tag{8}$$

The dissipation rate of turbulent kinetic energy, ε, is given by

$$\varepsilon = \nu \left\langle \frac{\partial u_i'}{\partial x_j} + \frac{\partial u_i'}{\partial x_j} \right\rangle . \tag{9}$$

In the k-ε model, by adopting dimensional arguments, turbulent kinematic viscosity is given by

$$\nu_t = c_\mu f_\mu \frac{\mathrm{k}^2}{\varepsilon} . \tag{10}$$

where c_μ is a model constant. The turbulent parameters, k and ε, are determined through the following transport equations

$$\frac{D\mathrm{k}}{Dt} = P - \varepsilon + \frac{\partial}{\partial x_i}\left(\frac{\nu_t}{\sigma_k} \frac{\partial k}{\partial x_i} \right), \tag{11}$$

$$\frac{D\varepsilon}{Dt} = \frac{\partial}{\partial x_i}\left(\frac{\nu_T}{\nu_\varepsilon} \frac{\partial \varepsilon}{\partial x_i} \right) + C_{\varepsilon 1} \frac{\varepsilon}{\mathrm{k}} P - c_{\varepsilon 2} \frac{\varepsilon^2}{\mathrm{k}} , \tag{12}$$

$$P = \nu_t \frac{\partial u_i}{\partial x_i} \left(\frac{\partial u_i}{\partial x_j} + \frac{\partial u_j}{\partial x_i} \right), \tag{13}$$

all the C's and σ's are model constants. Typical values of empirical constants are shown in Table 3.

Table 3 – Model Constants for k–ε two-equation model

C_μ	$C_{\varepsilon 1}$	$C_{\varepsilon 2}$	σ_k	σ_ε	Pr_T
0.09	1.44	1.92	1.0	1.3	0.9

The complete definition of the mathematical problem depends now only on the appropriate specification of the boundary conditions. At the wall, this is normally made with the help of wall functions. For the streamwise velocity component, u, the wall functions for k and for ε are

$$\frac{u}{u_\tau} = \frac{1}{\kappa} \ln(E_1 y^+), \quad y^+ = \frac{y u_\tau}{\nu}, \tag{14}$$

$$k = \frac{u_\tau^2}{(c_\mu)^{1/2}}, \tag{15}$$

$$\nu_t = c_\mu \frac{k^2}{\varepsilon}, \tag{16}$$

$$\varepsilon = \frac{u_\tau^3}{k\, y}, \tag{17}$$

where u and y should be evaluated in the fully turbulent region of the flow, κ is the von Karman constant (=0.4), E_1 is the linear coefficient of the law of the wall (=9) and u_τ is the skin friction velocity.

4. The Boundary Conditions

Flows that are apparently insensitive to the characteristic scale K, but depend on other global scale of the flow are termed flows over surfaces of the "D" type. In the latter case, the roughness is geometrically characterized by a surface with a series of closely spaced grooves within which the flow generates stable vortical configurations. To describe the part of the velocity profile that deviates from the logarithmic law in the defect region, in the flow region above the rough elements, the mean motion is considered to be independent of the characteristic scales associated with the near wall flow. Thus, the law of the wall for flows over rough surfaces can be written in a general form, valid both types of roughness as

$$\frac{u}{u_\tau} = \frac{1}{k} \ln \frac{(y_T + \in) u_\tau}{\nu} + A - \frac{\Delta u}{u_\tau}, \tag{18}$$

where,

$$\frac{\Delta u}{u_\tau} = \frac{1}{k} \ln \frac{\in u_\tau}{\nu} + C_i, \tag{19}$$

where the domain of validity is the fully turbulent region. It can be verified through application of the single limit concept of Kaplun(1967),(Silva Freire and Hirata(1990)).

In the above equations all symbols have their classical meaning; C_i , i= K, D is a constant characteristic of the type of roughness; the coordinate y_T is the distance measured from the crest of the roughness elements; $\in$ is the displacement in origin, referred to in literature as the error in origin as well.

For flows over rough surfaces the lower bound of the overlap regions must change, being a function of the surface geometry. The characteristic length scale for the near wall region must be the displacement in origin. It is also clear that, in either case, roughness of the type "K" or roughness of the type "D", the roughness elements penetrate well into the fully turbulent region so that the new origin for the velocity profile will always be located in the overlap fully turbulent region. Therefore, concerning the k - ε model, it appears that an adequate description of the flow can be given provided the wall boundary condition is written according with Eq.(18). Figure 5 is very representative of the phenomena of roughness at the wall influencing the energy transfer process, as in momentum exchange or in heat flow rate. In the Fig. 5, the distance between the two group of curves is the so mathematically described by the roughness function, Eq.(19) and analogically Eq.(21)

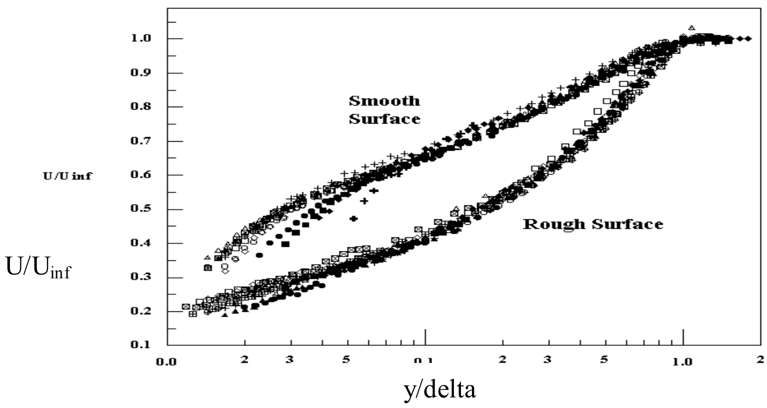

Figure 5 – Represents of the phenomena of the rough wall influencing the energy transfer process, as in momentum exchange or in heat flow rate.

Expressions (18) and (19) can be extended to the thermal turbulent boundary layer through asymptotic or dimensional arguments. Based on similarity arguments for transfer processes in turbulent flows, Silva Freire and Hirata(1990) proposed to write the temperature law of the wall as

$$\frac{T - T_w}{t_\tau} = \frac{1}{k_t} \ln \frac{\Pr (y_T + \in) u_\tau}{\nu} + B - \frac{\Delta T}{t_\tau} \tag{20}$$

where,

$$\frac{\Delta T}{t_\tau} = \frac{1}{k_t} \ln \frac{\Pr \in u_\tau}{\nu} + D_i \tag{21}$$

and D_i , *i*= K, D; is a constant characteristic of the roughness.

Equations (20) and (21) are the law of the wall formulation for flows over rough surfaces with transfer of heat, and will be used to specify the boundary conditions on a k–ε formulation of the problem.

4.1. The Displacement in Origin

The procedures for determination of the displacement in origin for the velocity profiles and temperature profiles was based on the Perry and Joubert(1963) method.

The determination of the displacement in origin is significant for the evaluation of the properties of the flow over a rough surface, including all local and global parameters. All graphical methods for its determination, however, assume the existence of a logarithmic region, which may not occur near to a step change in roughness. The estimated values of $\in t$ were obtained experimentally in Avelino(2000). In the numerical computations the expressions in Table 4 will be used to represent $\in t$.

In the same way as for the velocity profiles, to determine the displacement in origin, the temperature profiles were plotted in semi-log form, in dimensional coordinates. Next, the normal distance from the wall was incremented by 0.1mm and a straight line fit was applied to the resulting points. Searching for the maximum coefficient of determination, the best fit was determined. Other statistical parameters were also observed, as the residual sum of squares and the residual mean square.

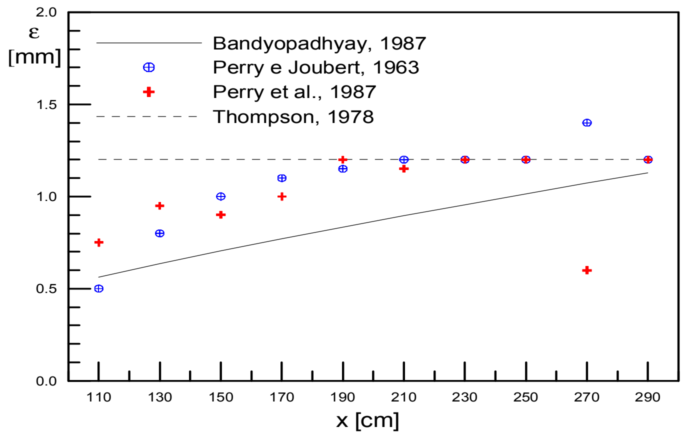

Figure 6 – Displacement in origin for temperature profiles - Type I rough surface.

It is seen the experimental data agree with this analytical result for the rough surface. Figure 6 present the error in origin for rough surface Type I.

5. Experimental Results and Discussion

5.1. Velocity Profile Data

The measured velocity profiles for the two different flow configurations are shown in Figs.7 and 8, in comparison with measured profiles for flow developing over smooth surface, which is adopted as the reference flow case. In Figs.7 and 8, the dashed line is the classical law of the wall, with κ=0.4, and A=5.0, or the particular case of the Eq.(1) when $\Delta u/u_\tau=0$. It is seen that the experimental data agree with this analytical result for the smooth surface. The comparison between the profiles developed over the rough surfaces and the reference case furnishes the mathematical value of the velocity roughness functions, $\Delta u/u_\tau$.

It is known that for turbulent boundary layers developing over rough surfaces, the logarithmic regions of the flow suffer a slight deformation to the left side. In fact, as we shall see, a very popular method to find $\in$ is based on a procedure to restore the lower portion of the velocity profile to a logarithmic profile.

The displacement in origin, $\in$, was estimated by four different procedures. In fact, the procedures of Perry and Joubert(1963) and Perry et al.(1987) are the most rigorous that can be found in literature so that the data resulting from them must be seen as reliable. The procedures of Thompson(1978) and Bandyopadhyay(1987) are more simplified so that the values of $\in$ obtained through them must be seen just as a first approximation.

In Perry and Joubert(1963) method, arbitrary values of $\in$ are added to the wall distance measured from the top of the roughness elements and a straight line is fitted to the log-law region. The value of $\in$ that furnishes the logarithmic region is then considered to be the correct value for the displacement in origin. The method of Perry et al.(1987) is more sophisticated, resorting to a cross plot of $\in$ vs. $2\Pi/\kappa$, where Π stands for Cole's wake profile.

Therefore, to determine the displacement in origin, the velocity profiles were plotted in semi-log form, in dimensional coordinates. Next, the normal distance from the wall was incremented by 0.1mm and a straight line fit was applied to the resulting points. Searching for the maximum coefficient of determination, the best fit was determined. Other statistical parameters were also observed, as the residual sum of squares and the residual mean square.

Having found $\in$, the gradient of the log-law is used to determine u_τ. Another method to determine u_τ is the momentum-integral equation. The latter method, however, is very sensitive to any three-dimensionality of the flow and the determination of the derivatives of the various mean flow parameters is less accurate. The cited methods depend on the evaluation of the derivatives.

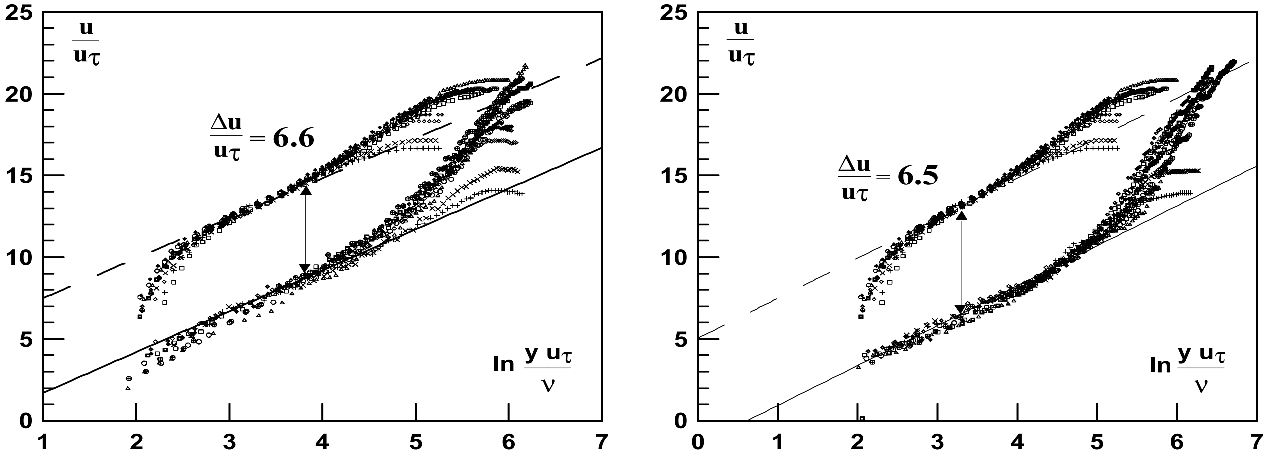

Figures 7 and 8 – Velocity profiles for the flows over smooth to rough surfaces in a plate.

Figures 7 and 8 show that $\in$ represents an evolution for the two considered rough surfaces, a fact that has been previously observed in 'K' type rough surfaces. The evolution of $\in$ on surfaces with more sparse rough elements is observed to be rather slower and representative of a 'D' type surface. In Figure 6, the value of $\in$ calculated through procedure suggested in Thompson(1978) furnishes $\in$=1.22. Antonia (1971,1972).

5.2. Temperature_Profile Data

Convective transfer of heat always involves transfer of momentum; therefore it is convenient to analyze temperature distributions on the basis of velocity distributions. Initially the temperature profiles were measured over a smooth surface in order to obtain a reference case, and to determine the temperature distributions in the law of the wall region. These results were then used to separately determine the displacement in origin and the temperature roughness function were investigated. Data from the original measurements of temperature profiles for the three different flow configurations are shown in Figs. 9 and 10.

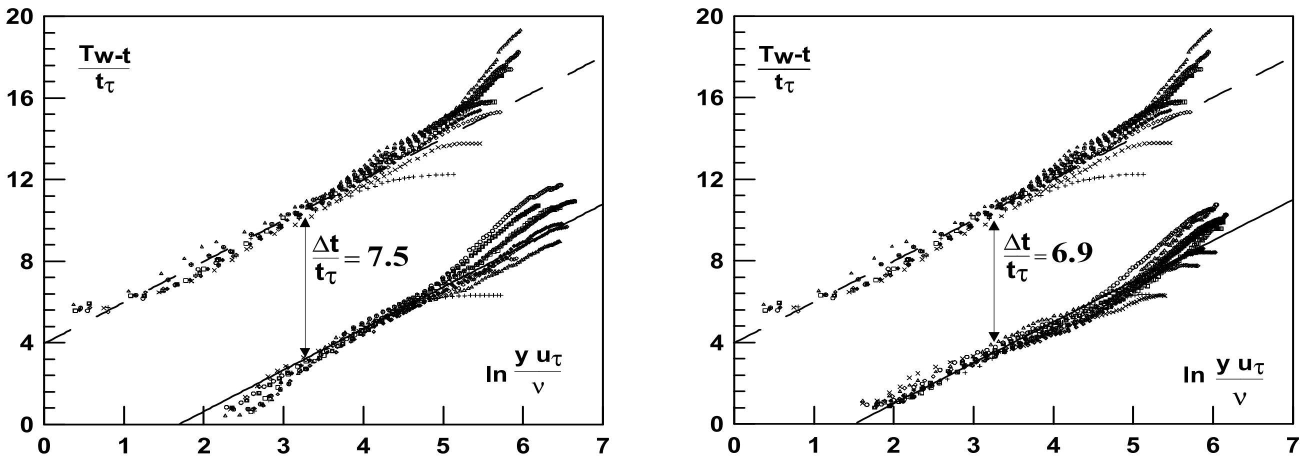

Figures 9 and 10 – Temperature profiles for the flows over smooth and Type III rough surfaces.

Table 4 – Behavior of displacement in origin and the roughness functions (Avelino, 2001).

Type of Surface	$\in$ (mm)	$\in_t$ (mm)	$\Delta u/u_\tau$	$\Delta t/t_\tau$
I	1.2	1.5	7.4	7.5
II	1.4	1.4	6.7	6.8
III	0.8	1.2	7.9	8.4

6. Summary and Conclusions

The increase in density of integrated circuits and the trend of miniaturization has significantly increased the problem of effective heat dissipation of microchips, making the use of microchannel cooling mandatory. The important conclusions of the literature survey are as follows:

- Convective heat transfer in microscale is significantly enhanced since the contact area between the IC chip and the coolant is increased, due to small size of the channel. The high thermal performance of the microscale heat sink is due to the fact that the heat transfer coefficient is inversely proportional to the length scale of the rough element.
- The geometric parameters have a significant influence on the convective heat transfer characteristics.
- There is a significant deviation in the behavior of convective heat transfer in microscale, than, observed in conventionally sized geometries.
- In addition to Re, Brinkman number also determine the flow regime boundaries from laminar-to-transition, and from transition-to-fully turbulent flow.

Microscale heat transfer has attracted researchers recently, due to the developments in the electronics and bioengineering industries. There are some fundamental differences between micro and macro heat transfer phenomenon. Although a substantial amount of experimental, analytical and numerical studies have been performed; there are still some points that are not yet understood, such as the boundaries of the transition from micro to macro and the boundary conditions for different flow conditions

The theory used here is based on late concepts by Nikuradse(1933), Clauser(1954) and Moore(1951), being extended to the thermal case through asymptotic and heuristic arguments, accounts for the effects of the changing in the surface conditions from one extensive uniform surface to another.

References

ANTONIA, R.A. and R.E.LUXTON, 1971. The Response of a Turbulent Boundary Layer to a Step Change in Surface Roughness Part 1. Smooth to Rough, *J. Fluid Mechanics*, Vol. 48, pp. 721-761.

ANTONIA, R.A. and R.E. LUXTON, 1972. The Response of a Turbulent Boundary Layer to a Step Change in Surface Roughness Part 2. Rough to Smooth, *J. Fluid Mechanics*, Vol. 53, pp. 734-757.

AVELINO, M.R., 2000. An Experimental/Numerical Study of the Turbulent Boundary Layer Development Along a Surface with a Sudden Change in Roughness, *J. of Braz. Soc. Mechanical Sciences*, Vol. XXII, No. 1, pp. 1-13.

BAYAZITOGLU, Y. and U. B. SATHUVALLI "Heat Transfer." *2004 Edition of CRC Engineering Handbook* (2003).

BRODERSEN, R.W., CHANDRAKASAN, A. and SHENG, S., Technologies for personal communications," Symp. on VLSI circuits, pp. 5–9, 1991.

CHANDRAKASAN, A.P., SHENG, S. and BRODERSEN, R. W., Low-power CMOS digital design," IEEE Journal of Solid-State Circuits, vol. 27, no. 4, pp. 473–484, April 1992.

CLAUSER, F.H., 1954. Turbulent Boundary Layers in Adverse Pressure Gradients*, J. Aero. Sci.*, Vol. 21, pp. 91.

GAD-EL-HAK, M. (Ed.), The MEMS Handbook, CRC Press, Boca Raton, FL, 2002.

GAD-EL-HAK, M., Transport phenomena in microdevices, Z. Angew. Math. Mech., Vol. 84, Issue 7 , Pp 494 – 498, 2003.

HERWIG, H., HAUSNER, O., Critical view on ‘‘new results in micro-fluid mechanics: an example, Int. J. Heat Mass Transfer 46 (2003) 935–937.

HERWIG, H., Flow and heat transfer in micro systems, Z. Angew. Math. Mech. 82 (2002) 579–586.

KAPLUN, S., 1967. *Fluid mechanics and singular perturbations*, Academic Press.

KARNIADAKIS, G.Em. BESKOK, A.Microflows: Fundamentals and Simulation, Springer-Verlag, New York, 2002.

KLINE, S.J, 1985. The Purpose of Uncertainty Analysis, *J. Fluids Engineering*, Vol. 107, pp. 153-160.

KNUDSEN, M., Die Gesetze der Molekularstrssomung und der inneren Reibungsstr€omung der Gase durch Rssohren, Annalen der Physik 28 (1909) 75–130.

LAUNDER, B.E. and SPALDING, D.B., 1974. The numerical Computation of Turbulent Flows, *Comp. Meth. Appl. Mech.*, Vol.3, pp. 269-289.

LIGRANI, P.M., R.J. MOFFAT and W.M. KAYS, 1979. The Thermal and Hydrodynamic Behavior of Thick Rough-Wall Turbulent Boundary Layers, *Report No. HMT-29*, Vol. 105, pp. 146-153.

LIGRANI, P.M., R.J. MOFFAT and W.M. KAYS, 1983. Artificially Thickened Turbulent Boundary Layers for Studying Heat and Skin-Friction on Rough Surfaces, *J. Fluids Engineering*, Stanford University.

MOORE, W.L., 1951. *An Experimental Investigation of the Boundary Layer Developing Along a Rough Surface*, Ph.D Thesis, State University of Iowa.

NIKURADSE, J., 1933. Stromungsgesetze in Rauhen Rohren, *V.D.I. Forshungsheft*, No. 361.

PERRY, A.E. and P.N. JOUBERT, 1963. Rough-Wall Boundary Layers in Adverse Pressure Gradients, *J. Fluid Mech.*, Vol. 17, pp. 193-211.

SILVA FREIRE, A.P., and M.H. HIRATA, 1990. Analysis of Thermal Turbulent Boundary Layers over Rough Surfaces, *Proc. III Brazilian Meeting on Thermal Sciences*, Florianopolis, pp. 313-316.

SPALDING, D.B., 1961. Heat Transfer to a Turbulent Stream from a Surface with Spanwise Discontinuity in Wall Temperature, *International Developments in Heta Transfer, ASME/Inst. of Mech. Engrs. Part II*, 439.